Matter

Article

Water-evaporation-induced direct current electricity generation based on stretchable hydrogel/Al_2O_3

Graphical abstract

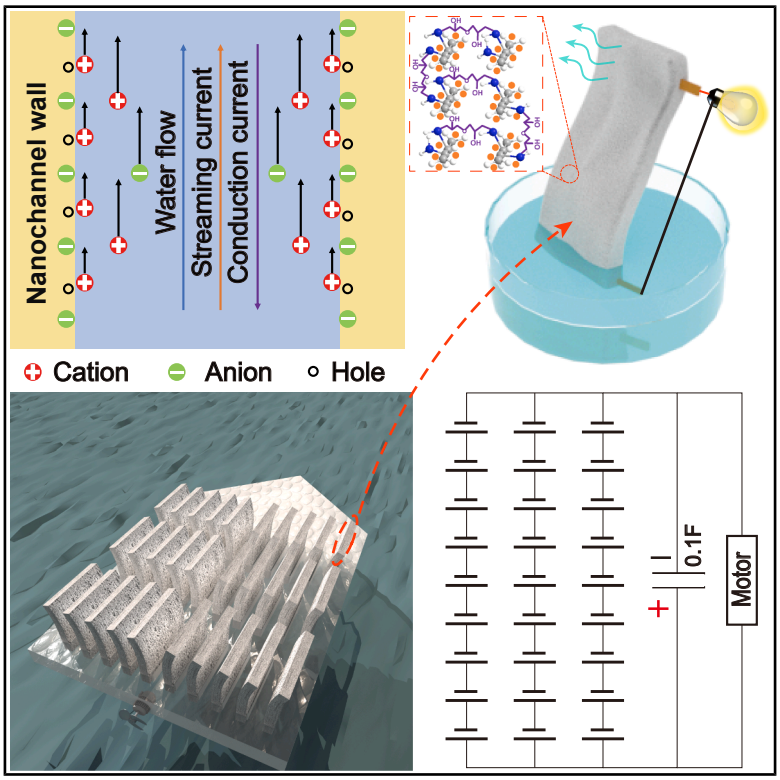

Highlights

- Flexible water-evaporation-induced harvester achieves 32 μA short-circuit current
- Porous gelatin/Al_2O_3/NaCl membranes maintain stable electrical output under stretching
- Scalable device architecture enables powering of commercial electronics

Authors

Chaoran Liu, Zai Wang, Xin Tong, ..., Linxi Dong, Gaofeng Wang, Zhong Lin Wang

Correspondence

liucr@hdu.edu.cn (C.L.), donglinxi@hdu.edu.cn (L.D.), zlwang@binn.cas.cn (Z.L.W.)

In brief

Liu et al. demonstrate a water-evaporation-induced high-direct-current electricity generator based on stretchable flexible hydrogel/Al2O3. This flexible hydrogel membrane can harvest energy from natural water evaporation, offering a low-cost and scalable solution for powering small electronics.

1 Discovery
A new material or phenomena

Liu et al., 2025, Matter 8, 102200
October 1, 2025
https://doi.org/10.1016/j.matt.2025.102200

CellPress

Please cite this article in press as: Liu et al., Water-evaporation-induced direct current electricity generation based on stretchable hydrogel/Al_2O_3, Matter (2025), https://doi.org/10.1016/j.matt.2025.102200

Matter

CellPress

Article

Water-evaporation-induced direct current electricity generation based on stretchable hydrogel/Al_2O_3

Chaoran Liu,[1,7,*] Zai Wang,[1] Xin Tong,[1] Zhenhua Wu,[2] Lin Zhou,[2] Haiyang Zou,[3] Ayodeji Ogunjuyibe,[4] Hongjian Lin,[5] Dongfang Yan,[1] Weihuang Yang,[1] Linxi Dong,[1,*] Gaofeng Wang,[1] and Zhong Lin Wang[6,*]

[1]Ministry of Education Engineering Research Center of Smart Microsensors and Microsystems, College of Electronics and Information, Hangzhou Dianzi University, Hangzhou 310018, P.R. China

[2]State Key Laboratory of Transducer Technology, Shanghai Institute of Microsystem and Information Technology, Chinese Academy of Sciences, Shanghai 200050, P.R. China

[3]College of Materials Science and Engineering, Sichuan University, Chengdu 610065, P.R. China

[4]Department of Electrical and Electronic Engineering, Faculty of Technology, University of Ibadan, Ibadan, Oyo State, Nigeria

[5]Department of Electrical Engineering, City University of Hong Kong, Hong Kong SAR 999077, P.R. China

[6]Beijing Institute of Nanoenergy and Nanosystems, Chinese Academy of Sciences, Beijing 101400, P.R. China

[7]Lead contact

*Correspondence: liucr@hdu.edu.cn (C.L.), donglinxi@hdu.edu.cn (L.D.), zlwang@binn.cas.cn (Z.L.W.)

https://doi.org/10.1016/j.matt.2025.102200

PROGRESS AND POTENTIAL In this work, a flexible and stretchable energy harvester based on a gelatin/Al_2O_3/NaCl hydrogel composite membrane was developed to address the challenges of low output and poor mechanical robustness in current water-evaporation-induced energy harvesting systems. Utilizing a simple and scalable sol-gel process, the porous hydrogel membrane exhibits excellent hydrophilicity, mechanical elasticity, and enhanced ionic conductivity. The device achieves a maximum short-circuit current of 32 μA and an open-circuit voltage of 0.4 V, with stable electrical performance under bending and stretching conditions. Systematic optimization of material composition, device dimensions, and ambient factors was carried out to maximize output. Practical demonstrations, including capacitor charging and powering commercial electronics, such as digital calculators, light-emitting diodes (LEDs), and hygrometers, validate the real-world applicability. Moreover, by assembling multiple units in series and parallel, the system successfully drove a motorized foam boat, highlighting the scalability of the energy output. The proposed hydrogel-based energy harvester offers a promising platform for sustainable, flexible, and low-power energy harvesting applications. Its low-cost fabrication, mechanical resilience, and modular integration capabilities make it highly suitable for next-generation self-powered wearable devices, environmental monitoring systems, and micro-robotics. Beyond individual applications, this system architecture provides a versatile foundation for hybrid energy harvesting networks, enabling distributed energy generation for Internet of Things (IoT) ecosystems and off-grid sensing. Future research will focus on enhancing long-term durability, exploring integration with energy storage elements, and expanding material platforms to further diversify application fields.

SUMMARY

Harvesting sustainable electricity from natural water evaporation has been attracting attention as a promising alternative to supply power for low-power systems. However, low-current output and rigid materials largely hinder its extensive applications. Herein, we present a water-evaporation-induced high-direct-current electricity generator based on stretchable flexible hydrogel/Al_2O_3. This flexible electricity generator forms a porous Al_2O_3 substrate by dissolving the NaCl from the heat-cured gelatin/Al_2O_3/NaCl. It achieves a sustainable and stable direct current of 32 μA, a low internal resistance of 5.18 kΩ, and a maximal output power of 1.76 μW with a maximum output power density of 0.55 mW m^{-2} by optimizing the electricity generator's physical dimensions and concentration ratios. The developed water-evaporation-induced electricity generator shows many application prospects, including as a power supply for digital calculators and hygrothermographs and to drive

Please cite this article in press as: Liu et al., Water-evaporation-induced direct current electricity generation based on stretchable hydrogel/Al_2O_3, Matter (2025), https://doi.org/10.1016/j.matt.2025.102200

a boat of 5.1 cm. This research provides an in-depth study on a stretchable high-direct-current water-evaporation-induced electricity generator and an efficient approach to power supplies for low-power systems.

INTRODUCTION

Renewable and clean environmental energy has become critical to the progress of human civilization, attributed to the rapid depletion of traditional non-renewable resources.[1,2] Harvesting energy from the environment offers a new solution to the growing energy crisis, which has developed rapidly in recent decades. Many feasible energy harvesting mechanisms, such as triboelectricity,[3–8] piezoelectricity,[9–11] thermoelectricity,[12–14] etc., have been presented to improve the output performance. Among these, a water-evaporation-induced electricity generator holds significant potential. The utilization of water energy has largely occurred on a macroscopic scale throughout human history, such as water flow driving turbines. This requires complex mechanical structures, resulting in high costs and potential environmental issues. Consequently, harvesting sustainable electricity

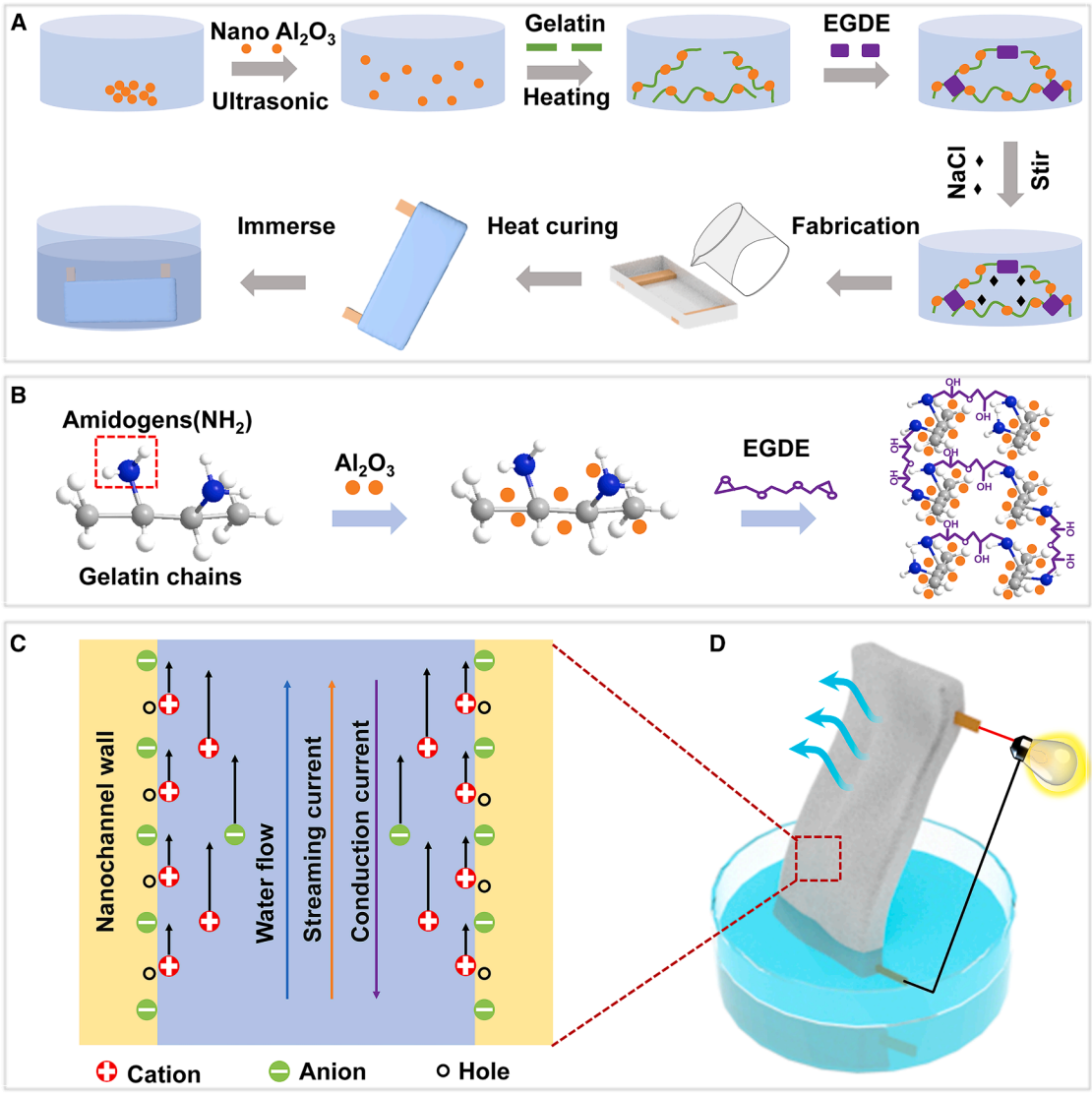

Figure 1. Preparation and working principle of the S-ENG

(A) Schematic diagram of S-ENG preparation process.

(B) The chemical formation process of S-ENG.

(C) Schematic of the water-flow-induced streaming current in a single nanochannel of the S-ENG.

(D) Working process of the S-ENG.

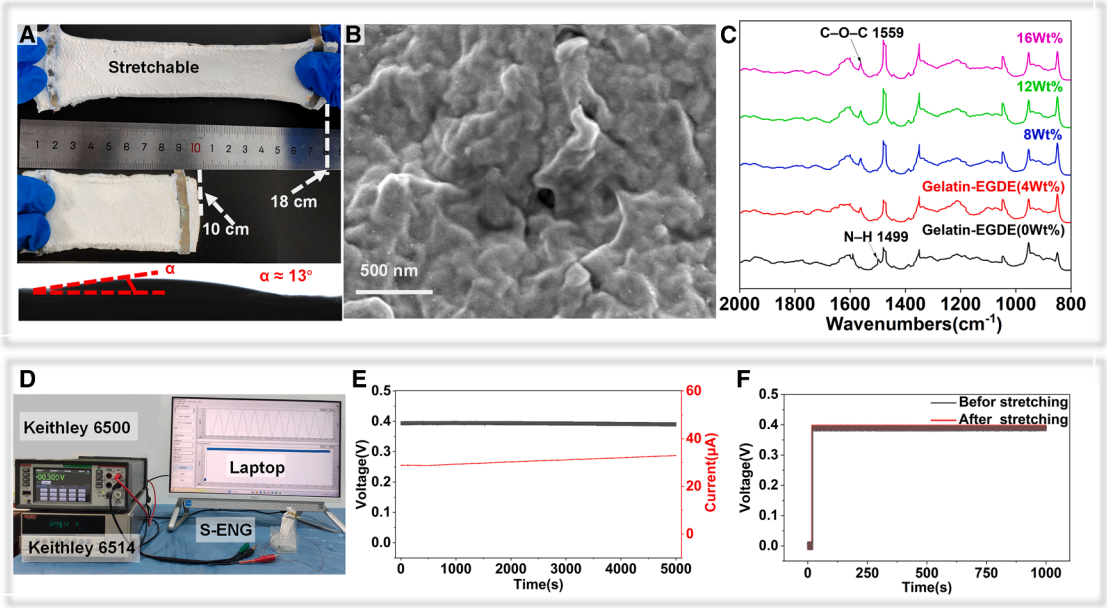

Figure 2. The chemical characterization and output testing of S-ENG

(A) Stretchable and hydrophilic S-ENG.

(B) Scanning electron microscopy (SEM) image of the S-ENG.

(C) FTIR spectra of gelatin films at different EGDE concentrations.

(D) Photo of the measurement system.

(E) Long-term stability of the output of the S-ENG with Al_2O_3, gelatin, and NaCl of 0.24, 0.20, and 0.25 g mL^{-1}, respectively, and dimensions of 80 × 40 × 2 mm^3 at room relative humidity ≈ 60.0% and temperature ≈ 25.0°C during the test.

(F) The voltage output before and after stretching.

from natural water evaporation has gained more attention due to its spontaneity, ubiquity, and direct current (DC) output.[15–18]

Various materials and elegant approaches have been reported for water-evaporation-induced power generation. In particular, Zhou et al. conducted a study in 2017 that demonstrated that water evaporation on functionalized porous carbon black films can reliably generate a sustained voltage of up to 1 V and a current of 100 nA.[19] Composite materials have also been proposed, such as carbon nanospheres and TiO_2 nanowires. The super-hydrophilic surface formed by combining TiO_2 nanowires with carbon materials demonstrated a voltage of 1.6 V and significantly enhanced power output.[20] These power-generating materials include inorganic carbons,[21–24] inorganic solid oxides,[25,26] organic polymers,[27–30] and some natural biological materials.[31–35] Their power generation levels and efficiencies vary significantly depending on the hydrophilicity and surface charge density of the materials. However, some common deficiencies, such as low-current output, limited stability, and rigid materials, hinder the water-evaporation-induced electricity generation performance and their widespread application significantly.

The high-direct-current water-evaporation-induced stretchable electricity nanogenerator (S-ENG) was designed based on flexible hydrogel/Al_2O_3, enabled by solid-liquid triboelectric nanogeneration. The optimized S-ENG achieves a continuous and stable DC output of 32 μA (voltage ≈ 0.4 V) and a maximal output power density of 0.55 mW m^{-2}. Stretchable hydrogel materials exhibit excellent mechanical properties, including pliability >270° (Figure S5) and ductility >80%. The current and voltage induced by evaporation are effectively enhanced by connecting multiple S-ENGs in series and parallel configurations. This emphasizes the potential applications of S-ENGs in water-evaporation-induced power generation.

RESULTS

Preparation of S-ENG

We present a preparation process for the S-ENG, as shown in Figure 1A. Firstly, we disperse 12 g Al_2O_3 with a particle size of ~250 nm (Figure S2) in 50 mL deionized water and ultrasonicate it for 30 min to create an Al_2O_3 nanoparticle suspension. Then, 10 g gelatin is added to the suspension and heated to 60°C with continuous stirring on a magnetic stirrer until fully dissolved. Subsequently, 2 mL ethylene glycol diglycidyl ether (EGDE) is added as a cross-linking agent. Al_2O_3 particles adsorb into the gelatin chains by the intermolecular forces.[36] Furthermore, the epoxide groups of EGDE link the amidogens (NH_2) of the adjacent gelatin chains, forming a composite hydrogel/Al_2O_3 mesh (Figure 1B).[37] Finally, 12.5 g NaCl particles are dissolved and embedded into the composite mesh. The mixed solution (8 mL) is poured into the mold and dried in an oven at 70°C for 3 h, forming the gelatin/Al_2O_3/NaCl film. The composite film with two stainless-steel mesh electrodes is solidified and molded. It forms the multi-porous structure by water dissolving the residual NaCl particles from the S-ENG film.

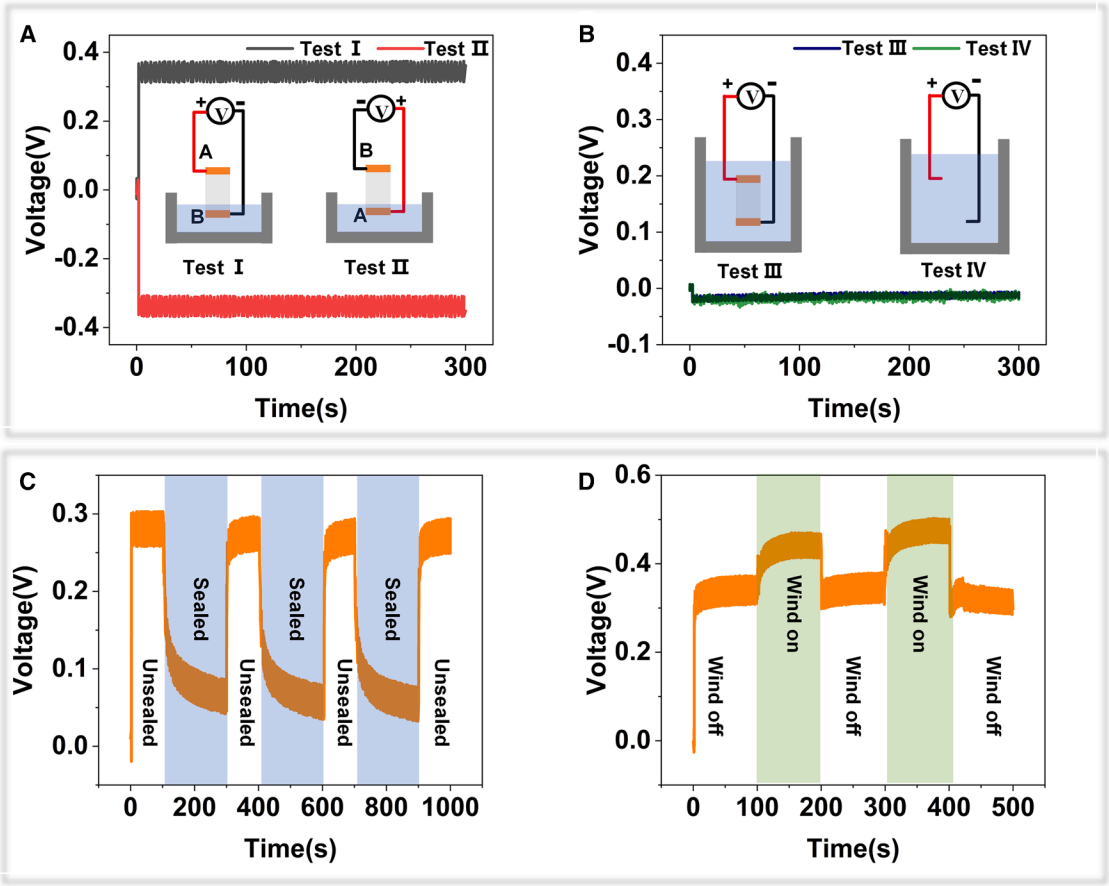

Figure 3. Experiments demonstrating the mechanism of water-evaporation-induced electricity generation

(A) Voltage generated by the device before (test I) and after (test II) the device is turned upside down.

(B) Test III: voltage of the device completely submerged in water. Test IV: voltage between two wires with the other ends immersed in water.

(C) Voltage of the device when the sink is periodically sealed and unsealed.

(D) Voltage of the device when the ambient air flow of 0.1 m s^{-1} is periodically turned on and off.

Working principle and experimental measurement

The as-fabricated S-ENG with a hydrophilic multi-porous structure continuously drives water flow climbing to the top electrode by the capillary force and water evaporation (Figures 1C and 1D). Water flows carrying the molecules and ions impact the porous hydrogel/Al_2O_3 surface owing to the thermal motion and liquid pressure based on the Wang model.[38,39] Electrons transfer between the solid atoms and water molecules attributing to the overlap of electron clouds between the solid atoms and water molecules. The hydrogel/Al_2O_3 gains electrons during the liquid-solid contact electrification process.[40] In addition, the ionization reaction of the oxygen-containing functional groups on the hydrogel/Al_2O_3 surface may occur simultaneously, leading to the generation of anions at the liquid-solid interface. Cations flowing in the water are attracted to the negatively charged surface of the nanochannels due to electrostatic interactions, forming an electric double layer (EDL).[41] The movement of ions within the EDL results in the transport of net positive charge under the capillary force driving the flows, forming the streaming current (Figure 1C).[42] Simultaneously, the induced electric field generated by the polarization of charges along the axial direction gives rise to a streaming potential. This potential difference drives electrons to move continuously through the external circuit, which leads to a reversed DC conduction current of this S-ENG. A stable electrical output is generated when the streaming current and conduction current approach equilibrium.[43]

The S-ENG also has remarkable ductility, stretching more than 80% (Figure 2A), and a hydrophilic porous structure (Figure 2B) with a stable output performance (Figures 2F and S3). Comparing the spectrum of gelatin with the spectrum of gelatin-EGDE, the absorption band at 1,499 cm^{-1} (belonging to the N–H deformation of primary amine groups on gelatin chains) nearly disappeared, implying that the epoxide group of EGDE has been coupled with the $–NH_2$ groups of gelatin. The peak at 1,559 cm^{-1} (assigned to the symmetric vibration of C–O–C stretching shifted in the gelatin-EGDE) appeared, demonstrating that the –OH groups of gelatin participated in the formation of ether bonds in the gelatin backbone (Figure 2C). The experimental setup for measuring the output performance of the S-ENG is shown in Figure 2D (Figure S4). The water flow quickly climbs along the S-ENG hydrophilic film as the bottom electrode is immersed in deionized water. The continuous flow climbing is induced by the evaporation above the waterline, which generates a potential difference between the

Please cite this article in press as: Liu et al., Water-evaporation-induced direct current electricity generation based on stretchable hydrogel/Al_2O_3, Matter (2025), https://doi.org/10.1016/j.matt.2025.102200

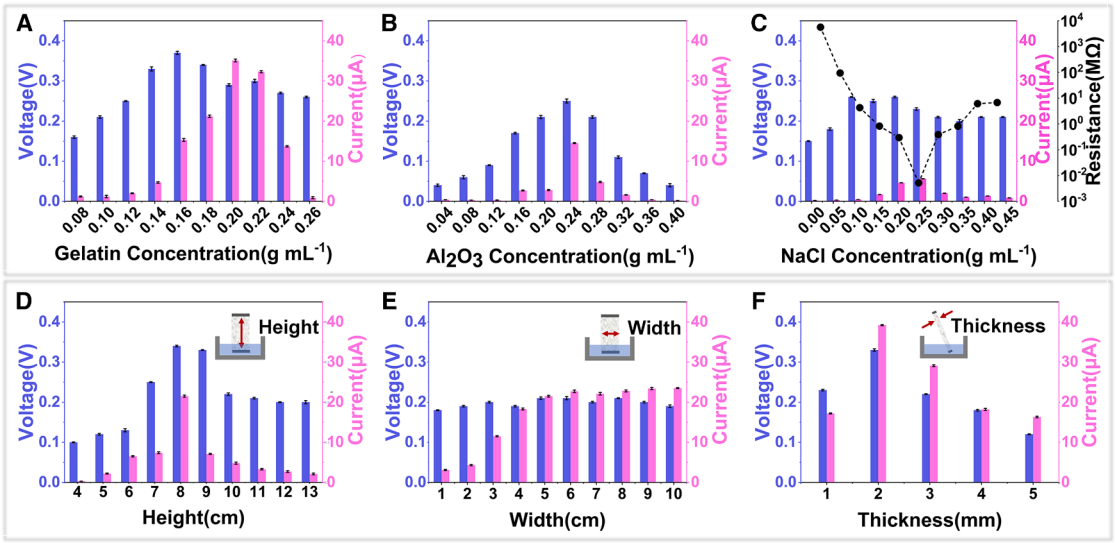

Figure 4. Effects of material concentrations and structural dimensions on the output performance of the gelatin/Al_2O_3/NaCl film

(A) Different gelatin concentrations (Al_2O_3: 0.20 g mL^{-1}, NaCl: 0.20 g mL^{-1}).

(B) Different Al_2O_3 concentrations (gelatin: 0.14 g mL^{-1}, NaCl: 0.20 g mL^{-1}

(C) Different NaCl concentrations (gelatin: 0.14 g mL^{-1}, Al_2O_3: 0.20 g mL^{-1}). Inset: the resistance of S-ENG varies with NaCl concentration.

(D) Different heights between two electrodes (width: 3 cm, thickness: 2 mm).

(E) Different widths (height: 8 cm, thickness: 2 mm).

(F) Different thicknesses (height: 8 cm, width: 3 cm).

two electrodes of the S-ENG. The as-fabricated S-ENG generates an open-circuit voltage of 0.4 V and a short-circuit current of 32 μA at room conditions, which have physical dimensions of 80 × 40 × 2 mm^3 and gelatin/Al_2O_3/NaCl concentrations of 0.20, 0.24, and 0.25 g mL^{-1}, respectively (Figure 2E). Except for deionized water, the S-ENG has output in all aqueous solutions (Figure S1).

To clarify the power generation mechanism, we conducted four contrast experiments labeled I–IV (Figures 3A and 3B). The output of the S-ENG exhibits obviously reversed polarity with an equivalent value as the top-bottom electrodes are overturned. There is no output voltage if the entire S-ENG is immersed in water. Tests I–IV verify that the mechanism of the S-ENG is water-evaporation-induced electricity generation rather than the primary battery effect. In addition, we further explore the influence of water evaporation in the S-ENG. Figure 3C shows the output voltage declining rapidly, nearly to 0 V, which results from the sealed sink increasing the inner humidity and inhibiting the water evaporation. The output voltage immediately rises to 0.3 V as the sealed film is removed. Commonly, wind airflow will facilitate water evaporation. The output voltage increases from 0.3 to 0.42 V when 0.1 m s^{-1} wind airflow is applied to the S-ENG and recovers to its initial value when the wind is off (Figure 3D). The sealed and wind-on/off experiments also demonstrate the water-evaporation-induced electricity generation mechanism of the S-ENG.

DISCUSSION

Electricity optimization

The material proportion and structural dimensions of S-ENG are further optimized to enhance output performance. According to the working principle, the zeta potential and the hydrophilicity of the materials are crucial to the output voltage, while the conductivity affects the output current (Equation S1).[20] Figures 4A–4C show the test results of the as-fabricated S-ENGs with different material concentrations of gelatin (0.08:0.02:0.26 g mL^{-1}), Al_2O_3 (0.04:0.04:0.40 g mL^{-1}), and NaCl (0.00:0.05:0.45 g mL^{-1}) under the same structure size (80 × 30 × 3 mm^3), temperature (25°C), and humidity (60%) conditions. The lower-concentration gelatin of S-ENG has fewer gelatin chains participating in interactions with water molecules and Al_2O_3, resulting in lower conductivity.[44] Therefore, the output performance is enhanced with the increase of gelatin concentration within an appropriate range, and the optimized gelatin concentration is 0.20 g mL^{-1}. Additionally, the Al_2O_3 concentration decides the zeta potential and conductivity of the gelatin/Al_2O_3/NaCl film.[45,46] The S-ENG has a maximal experimental output performance under an Al_2O_3 concentration of 0.24 g mL^{-1}. S-ENG is fabricated as the its film's multi-porous hydrophilic structure by washing out the NaCl particles.[47] The optimized NaCl concentration of the S-ENG film achieves a minimal internal resistance of 5.18 kΩ, which improves the output current. In addition, higher-concentration NaCl will reduce the zeta potential.[48]

As for structure dimensions, the width, thickness, and height of the S-ENG film impact the water evaporation velocity. As shown in Figure 4D, the evaporation area and the length of the nanochannels expand as the height increases, which significantly enhances both the output current and voltage. Further, lengthening the height reduces ion transport and the output voltage due to the insufficient capillary force driving the water flow. Widening the S-ENG film enhances the evaporation area and the total water flow volume, thereby improving the output

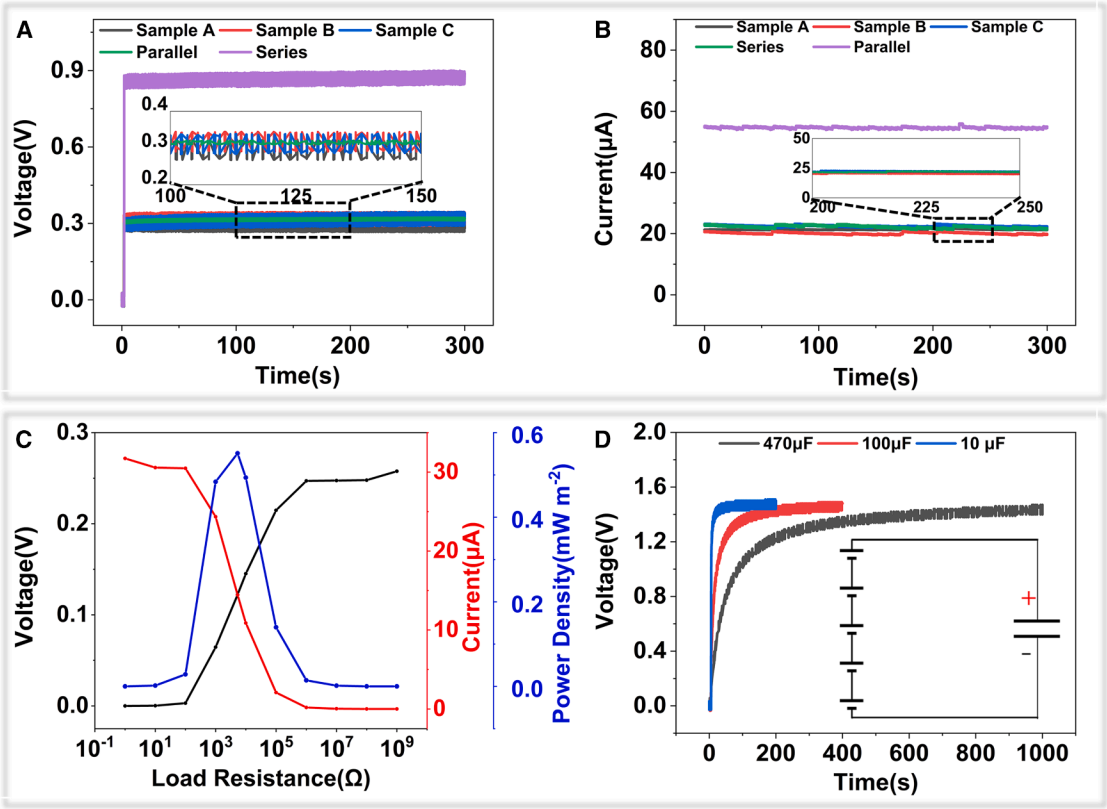

Figure 5. Output performance of S-ENGs

(A and B) Voltage (A) and current (B) of an individual sample and three samples in series or parallel.

(C) Output voltage, current, and power density of the S-ENG with different load resistances.

(D) The S-ENGs charging capacitors of 470, 100, and 10 μF. Inset: circuit diagram.

current, as expressed in Equation S2 and shown in Figure 4E. The voltage remains almost invariable owing to the vertical parallel nanochannels (Equation S2). It limits the amount of water flow and evaporation if the film is too thin, which declines the output performance (Figure 4F).[20]

Application

Enhancing the total output performance of a power supply is crucial for its applications. The power supply capacity can be improved by connecting multiple units in series or parallel. Figures 5A and 5B show the experimental results that the voltage has been boosted nearly triple by connecting the three S-ENGs in series, as well as the current in paralleling connection. The optimized single S-ENG achieves a maximal output power density of 0.55 mW m^{-2} with a maximal output current of 32 μA (Figure 5C). Five series S-ENGs enable charging different capacitors (10, 100, and 470 μF) up to 1.5 V quickly (Figure 5D).

Based on the remarkable power supply capacity, we further explore the potential applications of the stretchable evaporation-induced electricity nanogenerator. Figures 6A and 6B show that the series connection of eight S-ENGs enables the continuous powering of an electronic calculator with a sustained and stable output voltage of about 1.5 V (Video S1; supplemental information). Easily, the strong power supply ability of S-ENGs permanently lights a commercial light-emitting diode (LED) and a thermohygrometer via 4,700 μF capacitors without powering voltage decline (Video S2; supplemental information; Figures 6C–6F). We also explore the novel application of driving a boat using our as-fabricated S-ENGs. Figures 6G and 6H demonstrate that 30 S-ENGs in series/parallel can power a motor to drive a foam boat 5.1 cm (Video S3; supplemental information). The above experiments indicate that the developed S-ENG achieves stable direct-current electricity generation and enables powering micro-electronic devices or systems.

METHODS

Materials: gelatin and NaCl were purchased from Aladdin (Shanghai, China). EGDE was purchased from Kuer Bioengineering (Hefei, China). Al_2O_3 was purchased from Macklin (China).

Characterization of S-ENGs: the morphologies of the S-ENG were characterized by scanning electron microscopy (ZEISS Sigma 300). The Fourier transform infrared spectra (FTIR spectra) of the S-ENG were characterized by an FTIR spectrometer (VERTEX 70). Static contact angle tests were performed using an optical contact angle measuring system (PZ-200SD).

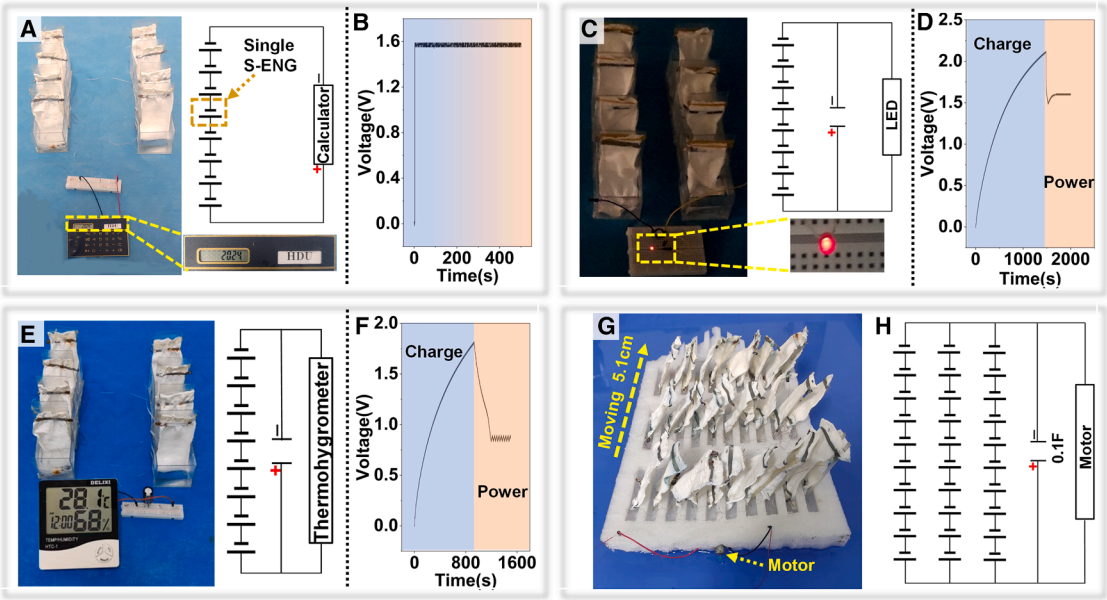

Figure 6. Applications of S-ENGs

(A) Eight series-connected S-ENGs power an electronic calculator and its equivalent circuit.
(B) The output voltage.
(C) Eight series-connected S-ENGs power an LED with a 4,700 μF capacitor and its equivalent circuit.
(D) The powering voltage of the 4,700 μF capacitor.
(E) Eight series-connected S-ENGs power a thermohygrometer with a 4,700 μF capacitor and its equivalent circuit.
(F) The powering voltage of the 4,700 μF capacitor.
(G) Photo of the foam boat powered by 30 S-ENGs connected in series/parallel.
(H) The equivalent circuit for driving the foam boat.

Output voltage and current were recorded by a Keithley 6514 and Keithley 6500, with data transmitted to a laptop for real-time analysis. A Testo 605i humidity and temperature meter and a Testo 405-V1 anemometer were used to measure relative humidity, temperature, and air flow velocity, respectively.

RESOURCE AVAILABILITY

Lead contact

Further information and requests for resources and reagents should be directed to and will be fulfilled by the lead contact, Chaoran Liu (liucr@hdu.edu.cn).

Materials availability

All materials are available upon request from the authors.

Data and code availability

Data are available upon request from the authors.

ACKNOWLEDGMENTS

This work was supported in part by the National Key R&D Program of China (no. 2022YFB3204800), the Fundamental Research Funds for the Provincial Universities of Zhejiang (no. GK249909299001-003), the Zhejiang Provincial Talent Project under grant no. 2021R2009, and the National Natural Science Foundation of China (no. 92373202).

AUTHOR CONTRIBUTIONS

C.L. and Z. Wang performed the experiment and analyzed the data. X.T. and C.L. fabricated the S-ENG and accomplished characterization. Z. Wu, L.Z., H.Z., A.O., H.L., W.Y., and G.W. provided valuable advice in the S-ENG system. C.L., L.D., and Z.L.W. initialized the idea, designed the experiment, and analyzed the idea.

DECLARATION OF INTERESTS

The authors declare no competing interests.

SUPPLEMENTAL INFORMATION

Supplemental information can be found online at https://doi.org/10.1016/j.matt.2025.102200.

Received: February 16, 2025
Revised: April 17, 2025
Accepted: May 15, 2025

REFERENCES

1. Narwal, S., Kaur, M., Yadav, D.S., and Bast, F. (2024). Sustainable blue economy: Opportunities and challenges. J. Biosci. *49*, 18. https://doi.org/10.1007/s12038-023-00375-x.
2. Ryu, H., Yoon, H.J., and Kim, S.W. (2019). Hybrid energy harvesters: toward sustainable energy harvesting. Adv. Mater. *31*, 1802898. https://doi.org/10.1002/adma.201802898.
3. Liu, C., Tong, X., Wang, Z., Lin, H., Ogunjuyibe, A., Zou, H., Wu, Z., Liu, W., Yan, D., Ma, B., et al. (2025). Broadband and low-crest-factor direct-current triboelectric nanogenerator with phase-shifting modulation. Cell Rep. Phys. Sci. *6*, 102596. https://doi.org/10.1016/j.xcrp.2025.102596.
4. Li, Y., Liu, C., Zou, H., Che, L., Sun, P., Yan, J., Liu, W., Xu, Z., Yang, W., Dong, L., et al. (2023a). Integrated wearable smart sensor system for

real-time multi-parameter respiration health monitoring. Cell Rep. Phys. Sci. *4*, 101191. https://doi.org/10.1016/j.xcrp.2022.101191.

5. Li, Y., Yu, J., Wei, Y., Wang, Y., Feng, Z., Cheng, L., Huo, Z., Lei, Y., and Sun, Q. (2023b). Recent progress in self-powered wireless sensors and systems based on TENG. Sensors *23*, 1329. https://doi.org/10.3390/s23031329.
6. Liu, C., Wang, Y., Zhang, N., Yang, X., Wang, Z., Zhao, L., Yang, W., Dong, L., Che, L., Wang, G., and Zhou, X. (2020). A self-powered and high sensitivity acceleration sensor with VQa model based on triboelectric nanogenerators (TENGs). Nano Energy *67*, 104228. https://doi.org/10.1016/j.nanoen.2019.104228.
7. Liu, C., Zhang, N., Li, J., Dong, L., Wang, T., Wang, Z., Wang, G., Zhou, X., and Zhang, J. (2019). Harvesting ultralow frequency (< 1 Hz) mechanical energy using triboelectric nanogenerator. Nano Energy *65*, 104011. https://doi.org/10.1016/j.nanoen.2019.104011.
8. Qu, H., Wan, L., Tian, Z., Liu, G., and Wang, Z.L. (2024). Evaporation Triboelectric-Nanogenerator: Harvesting Low-Grade Heat Energy from Ambient Environment. Adv. Mater. Technol. *9*, 2301409. https://doi.org/10.1002/admt.202301409.
9. Chorsi, M.T., Curry, E.J., Chorsi, H.T., Das, R., Baroody, J., Purohit, P.K., Ilies, H., and Nguyen, T.D. (2019). Piezoelectric biomaterials for sensors and actuators. Adv. Mater. *31*, 1802084. https://doi.org/10.1002/adma.201802084.
10. Ju, M., Dou, Z., Li, J.-W., Qiu, X., Shen, B., Zhang, D., Yao, F.-Z., Gong, W., and Wang, K. (2023). Piezoelectric materials and sensors for structural health monitoring: fundamental aspects, current status, and future perspectives. Sensors *23*, 543. https://doi.org/10.3390/s23010543.
11. Pierre Claver, U., and Zhao, G. (2021). Recent progress in flexible pressure sensors based electronic skin. Adv. Eng. Mater. *23*, 2001187. https://doi.org/10.1002/adem.202001187.
12. Haque, M.A., Kee, S., Villalva, D.R., Ong, W.L., and Baran, D. (2020). Halide perovskites: thermal transport and prospects for thermoelectricity. Adv. Sci. *7*, 1903389. https://doi.org/10.1002/advs.201903389.
13. Liu, K., Ding, T., Li, J., Chen, Q., Xue, G., Yang, P., Xu, M., Wang, Z.L., and Zhou, J. (2018). Thermal–electric nanogenerator based on the electrokinetic effect in porous carbon film. Adv. Energy Mater. *8*, 1702481. https://doi.org/10.1002/aenm.201702481.
14. Mu, X., Zhou, J., Wang, P., Chen, H., Yang, T., Chen, S., Miao, L., and Mori, T. (2022). A robust starch–polyacrylamide hydrogel with scavenging energy harvesting capacity for efficient solar thermoelectricity–freshwater cogeneration. Energy Environ. Sci. *15*, 3388–3399. https://doi.org/10.1039/d2ee01394k.
15. Lin, Z.-H., Cheng, G., Lee, S., Pradel, K.C., and Wang, Z.L. (2014). Harvesting water drop energy by a sequential contact-electrification and electrostatic-induction process. Adv. Mater. *26*, 4690–4696. https://doi.org/10.1002/adma.201400373.
16. Xu, W., Zheng, H., Liu, Y., Zhou, X., Zhang, C., Song, Y., Deng, X., Leung, M., Yang, Z., Xu, R.X., et al. (2020). A droplet-based electricity generator with high instantaneous power density. Nature *578*, 392–396. https://doi.org/10.1038/s41586-020-1985-6.
17. Yin, J., Zhang, Z., Li, X., Yu, J., Zhou, J., Chen, Y., and Guo, W. (2014). Waving potential in graphene. Nat. Commun. *5*, 3582. https://doi.org/10.1038/ncomms4582.
18. Zhao, Y., Song, L., Deng, K., Liu, Z., Zhang, Z., Yang, Y., Wang, C., Yang, H., Jin, A., Luo, Q., et al. (2008). Individual water-filled single-walled carbon nanotubes as hydroelectric power converters. Adv. Mater. *20*, 1772–1776. https://doi.org/10.1002/adma.200702956.
19. Xue, G., Xu, Y., Ding, T., Li, J., Yin, J., Fei, W., Cao, Y., Yu, J., Yuan, L., Gong, L., et al. (2017). Water-evaporation-induced electricity with nanostructured carbon materials. Nat. Nanotechnol. *12*, 317–321. https://doi.org/10.1038/NNANO.2016.300.
20. Ji, B., Chen, N., Shao, C., Liu, Q., Gao, J., Xu, T., Cheng, H., and Qu, L. (2019). Intelligent multiple-liquid evaporation power generation platform using distinctive Jaboticaba-like carbon nanosphere@ TiO_2 nanowires. J. Mater. Chem. A *7*, 6766–6772. https://doi.org/10.1039/c8ta12328d.
21. Li, Q., Zhou, M., Yang, Q., Yang, M., Wu, Q., Zhang, Z., and Yu, J. (2018). Flexible carbon dots composite paper for electricity generation from water vapor absorption. J. Mater. Chem. A *6*, 10639–10643. https://doi.org/10.1039/c8ta02505c.
22. Yang, P., Liu, K., Chen, Q., Li, J., Duan, J., Xue, G., Xu, Z., Xie, W., and Zhou, J. (2017). Solar-driven simultaneous steam production and electricity generation from salinity. Energy Environ. Sci. *10*, 1923–1927. https://doi.org/10.1039/c7ee01804e.
23. Zhang, G., Duan, Z., Qi, X., Xu, Y., Li, L., Ma, W., Zhang, H., Liu, C., and Yao, W. (2019). Harvesting environment energy from water-evaporation over free-standing graphene oxide sponges. Carbon *148*, 1–8. https://doi.org/10.1016/j.carbon.2019.03.041.
24. Zhao, F., Wang, L., Zhao, Y., Qu, L., and Dai, L. (2017). Graphene oxide nanoribbon assembly toward moisture-powered information storage. Adv. Mater. *29*, 1604972. https://doi.org/10.1002/adma.201604972.
25. Qin, Y., Wang, Y., Sun, X., Li, Y., Xu, H., Tan, Y., Li, Y., Song, T., and Sun, B. (2020). Constant electricity generation in nanostructured silicon by evaporation-driven water flow. Angew. Chem. *59*, 10619–10625. https://doi.org/10.1002/anie.202002762.
26. Shen, D., Xiao, M., Zou, G., Liu, L., Duley, W.W., and Zhou, Y.N. (2018). Self-powered wearable electronics based on moisture enabled electricity generation. Adv. Mater. *30*, 1705925. https://doi.org/10.1002/adma.201705925.
27. Li, L., Chen, Z., Hao, M., Wang, S., Sun, F., Zhao, Z., and Zhang, T. (2019). Moisture-driven power generation for multifunctional flexible sensing systems. Nano Lett. *19*, 5544–5552. https://doi.org/10.1021/acs.nanolett.9b02081.
28. Luo, Z., Liu, C., and Fan, S. (2019). A moisture induced self-charging device for energy harvesting and storage. Nano Energy *60*, 371–376. https://doi.org/10.1016/j.nanoen.2019.03.073.
29. Nie, X., Ji, B., Chen, N., Liang, Y., Han, Q., and Qu, L. (2018). Gradient doped polymer nanowire for moistelectric nanogenerator. Nano Energy *46*, 297–304. https://doi.org/10.1016/j.nanoen.2018.02.012.
30. Yang, W., Li, X., Han, X., Zhang, W., Wang, Z., Ma, X., Li, M., and Li, C. (2020). Asymmetric ionic aerogel of biologic nanofibrils for harvesting electricity from moisture. Nano Energy *71*, 104610. https://doi.org/10.1016/j.nanoen.2020.104610.
31. Das, S.S., Pedireddi, V.M., Bandopadhyay, A., Saha, P., and Chakraborty, S. (2019). Electrical power generation from wet textile mediated by spontaneous nanoscale evaporation. Nano Lett. *19*, 7191–7200. https://doi.org/10.1021/acs.nanolett.9b02783.
32. Li, M., Zong, L., Yang, W., Li, X., You, J., Wu, X., Li, Z., and Li, C. (2019). Biological nanofibrous generator for electricity harvest from moist air flow. Adv. Funct. Mater. *29*, 1901798. https://doi.org/10.1002/adfm.201901798.
33. Liu, X., Gao, H., Ward, J.E., Liu, X., Yin, B., Fu, T., Chen, J., Lovley, D.R., and Yao, J. (2020). Power generation from ambient humidity using protein nanowires. Nature *578*, 550–554. https://doi.org/10.1038/s41586-020-2010-9.
34. Mandal, S., Roy, S., Mandal, A., Ghoshal, T., Das, G., Singh, A., and Goswami, D.K. (2020). Protein-based flexible moisture-induced energy-harvesting devices as self-biased electronic sensors. ACS Appl. Electron. Mater. *2*, 780–789. https://doi.org/10.1021/acsaelm.9b00842.
35. Yang, W., Lv, L., Li, X., Han, X., Li, M., and Li, C. (2020). Quaternized silk nanofibrils for electricity generation from moisture and ion rectification. ACS Nano *14*, 10600–10607. https://doi.org/10.1021/acsnano.0c04686.
36. Sobhani, M., Tavakoli, H., Chermahini, M.D., and Kazazi, M. (2019). Preparation of macro-mesoporous γ-alumina via biology gelatin assisted aqueous sol-gel process. Ceram. Int. *45*, 1385–1391. https://doi.org/10.1016/j.ceramint.2018.09.056.

37. Kang, M., Liang, H., Hu, Y., Wei, Y., and Huang, D. (2024). Gelatin-based hydrogels with tunable network structure and mechanical property for promoting osteogenic differentiation. Int. J. Biol. Macromol. *281*, 136312. https://doi.org/10.1016/j.ijbiomac.2024.136312.

38. Lin, S., Xu, L., Chi Wang, A., and Wang, Z.L. (2020). Quantifying electron-transfer in liquid-solid contact electrification and the formation of electric double-layer. Nat. Commun. *11*, 399. https://doi.org/10.1038/s41467-019-14278-9.

39. Nie, J., Ren, Z., Xu, L., Lin, S., Zhan, F., Chen, X., and Wang, Z.L. (2020). Probing contact-electrification-induced electron and ion transfers at a liquid–solid interface. Adv. Mater. *32*, 1905696. https://doi.org/10.1002/adma.201905696.

40. Chi, J., Liu, C., Che, L., Li, D., Fan, K., Li, Q., Yang, W., Dong, L., Wang, G., and Wang, Z.L. (2022). Harvesting Water-Evaporation-Induced Electricity Based on Liquid–Solid Triboelectric Nanogenerator. Adv. Sci. *9*, 2201586. https://doi.org/10.1002/advs.202201586.

41. Huang, Y., Cheng, H., and Qu, L. (2021). Emerging materials for water-enabled electricity generation. ACS Mater. Lett. *3*, 193–209. https://doi.org/10.1021/acsmaterialslett.0c00474.

42. Zhang, R., Wang, S., Yeh, M.H., Pan, C., Lin, L., Yu, R., Zhang, Y., Zheng, L., Jiao, Z., and Wang, Z.L. (2015). A streaming potential/current-based microfluidic direct current generator for self-powered nanosystems. Adv. Mater. *27*, 6482–6487. https://doi.org/10.1002/adma.201502477.

43. Li, L., Hao, M., Yang, X., Sun, F., Bai, Y., Ding, H., Wang, S., and Zhang, T. (2020). Sustainable and flexible hydrovoltaic power generator for wearable sensing electronics. Nano Energy *72*, 104663. https://doi.org/10.1016/j.nanoen.2020.104663.

44. Kang, B.-C., Park, S.-J., Choi, H.-J., and Ha, T.-J. (2022). All-solution-processed wearable moist-electric generators based on engineered nanocomposites of carbon nanotube and gelatin incorporated with PEDOT:PSS interfacial blocking layer. Nano Energy *104*, 107890. https://doi.org/10.1016/j.nanoen.2022.107890.

45. Minakov, A.V., Pryazhnikov, M.I., Simunin, M.M., Dobrosmyslov, S.S., Kular, A.A., Molokeev, M.S., Volochaev, M.N., Khartov, S.V., and Voronin, A.S. (2022). Rheological properties of colloidal suspensions of alumina nanofibers. J. Mol. Liq. *367*, 120385. https://doi.org/10.1016/j.molliq.2022.120385.

46. Zawrah, M.F., Khattab, R.M., Girgis, L.G., El Daidamony, H., and Abdel Aziz, R.E. (2016). Stability and electrical conductivity of water-base Al_2O_3 nanofluids for different applications. HBRC j *12*, 227–234. https://doi.org/10.1016/j.hbrcj.2014.12.001.

47. Lee, S.B., Kim, Y.H., Chong, M.S., Hong, S.H., and Lee, Y.M. (2005). Study of gelatin-containing artificial skin V: fabrication of gelatin scaffolds using a salt-leaching method. Biomaterials *26*, 1961–1968. https://doi.org/10.1016/j.biomaterials.2004.06.032.

48. Zhao, Y., Xing, W., Xu, N., and Wong, F.-S. (2005). Effects of inorganic electrolytes on zeta potentials of ceramic microfiltration membranes. Sep. Purif. Technol. *42*, 117–121. https://doi.org/10.1016/j.seppur.2004.06.011.